Volume 7
Number 2
February 1, 1968

Inorganic Chemistry

CONTRIBUTION FROM THE DEPARTMENT OF CHEMISTRY,
PRINCETON UNIVERSITY, PRINCETON, NEW JERSEY 08540

Normal Coordinate Analysis for $Bi_6(OH)_{12}^{6+}$. Evidence for Bismuth–Bismuth Bonding[1a]

BY VICTOR A. MARONI[1b] AND THOMAS G. SPIRO

Received June 13, 1967

The vibrational spectrum of $Bi_6(OH)_{12}^{6+}$ has been subjected to a normal coordinate analysis, based on a cuboctahedral structure for this species. The known Bi–Bi and Bi–O distances in solution were used to construct the *G* matrix. Agreement with experiment was readily obtained using valence force constants which were of reasonable magnitude and fewer in number than the observable frequencies. The most economical fit, and also the best separation of the internal coordinates in the normal modes, was obtained if an attractive interaction between bismuth atoms was assumed. The hypothesis of bismuth–bismuth bonding is supported by the anomalously high intensity observed for the low-frequency Raman bands attributable to vibrations of the bismuth cage. A qualitative bonding scheme for the complex is suggested, which involves mutual overlap of sp hydrid orbitals on the bismuths.

Introduction

Recently we reported the Raman spectrum of the polynuclear hydroxybismuth(III) species, $Bi_6(OH)_{12}^{6+}$, both in solution and in the solid state, as well as the solid-state infrared spectrum.[2,3] Previously Danforth, Levy, and Agron[4] had carried out an X-ray scattering study of concentrated solutions of this species and had concluded from the resulting radial distribution function that the six bismuths are located at the corners of a regular octahedron with the twelve hydroxyl groups on the octahedral edges. The resulting structure, shown in Figure 1, is a nearly regular cuboctahedron with each bismuth atom lying just above the plane of four oxygen atoms. Qualitatively the observed Raman and infrared bands were in good accord with the proposed structure. We now report the results of a normal coordinate analysis of the vibrational spectrum, undertaken to determine whether quantitative predictions of the observed frequencies could be made on the basis of this structure and, if so, to examine the nature of the requisite force field.

We have found that the observed frequencies can indeed be predicted to within experimental error and with fewer force constants assumed than the number of frequencies observed. The required force constant for bismuth–oxygen stretching is of a reasonable magnitude and not sensitive to small variations in the somewhat uncertain position of the oxygen atoms. More interestingly, there appear to be strong grounds for suspecting that a significant amount of electron density is shared among the bismuth atoms, *i.e.*, that there is some degree of metal–metal bonding in the complex. Not only are fewer parameters required to fit the observed frequencies if a direct bismuth–bismuth interaction is included among them, but also this interaction is the primary contributor to three of the observed bands. The anomalously high intensity of these bands in the Raman spectrum may then be understood on the basis of the polarizability change involved in stretching bismuth–bismuth bonds. A qualitative molecular orbital scheme can be drawn up which includes such bonds in a reasonable manner.

Band Assignments

The representation of the Raman- and infrared-active normal vibrations for octahedral $Bi_6(OH)_{12}^{6+}$ (neglecting hydrogen atoms) is $2A_{1g} + 3E_g + 3F_{2g} + 4F_{1u}$. The A_{1g}, E_g, and F_{2g} modes are Raman active while the F_{1u} modes are infrared active. In the Raman spectrum seven of the eight expected bands are observed. Although eight bands were reported,[2] we have since concluded that the weak band at 148 cm^{-1} is an artifact of our instrument. The A_{1g} modes could be readily identified from polarization measurements. There was

(1) (a) This investigation was supported by Public Health Service Grant GM-13498, from the National Institute of General Medical Sciences; (b) NASA Predoctoral Fellow.

(2) V. A. Maroni and T. G. Spiro, *J. Am. Chem. Soc.*, **88**, 1410 (1966).

(3) It has since come to our attention that a preliminary Raman study of hydrolyzed bismuth perchlorate solutions was previously reported by A. Olin, *Svensk. Kem. Tidskr.*, **73**, 498 (1961). He listed five lines below 400 cm^{-1} in good agreement with our frequencies. The lines above 400 cm^{-1} were apparently not distinguished from the 460-cm^{-1} ClO_4^- band in his study.

(4) M. D. Danforth, H. A. Levy, and P. A. Agron, *J. Chem. Phys.*, **31**, 1458 (1959).

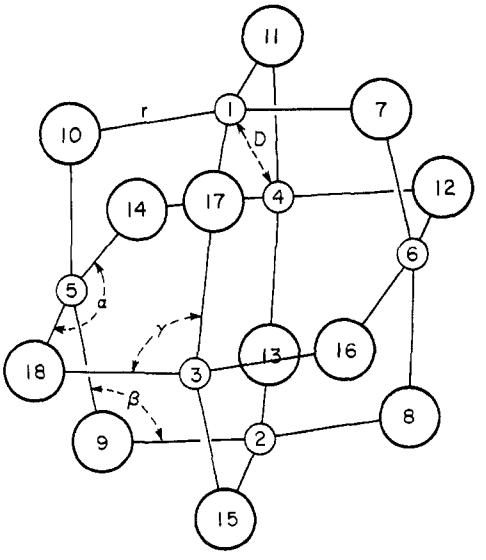

Figure 1.—Arrangement of bismuth atoms (small circles) and oxygen atoms (large circles) in the model assumed for $Bi_6(OH)_{12}^{6+}$. Parameters:[4] r = 2.33 Å, D = 3.71 Å, α = 164°, β = 106°, γ = 87°.

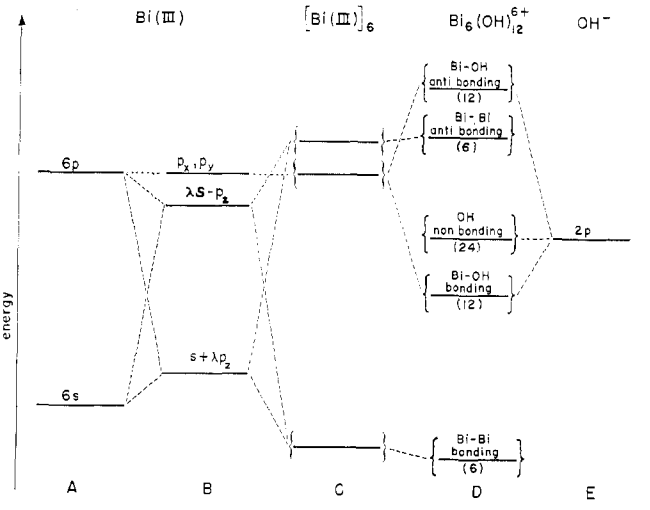

Figure 2.—Qualitative energy level scheme proposed for $Bi_6(OH)_{12}^{6+}$ (see text). Numbers in parentheses refer to the number of molecular orbitals of each type.

no basis for assigning the remaining Raman modes to E_g or F_{2g} symmetry and the present assignment of these is based on the normal coordinate analysis. We find that the 434- and 406-cm^{-1} bands can be interchanged in all of our calculations with only slight effect on the resultant force constants.

In the infrared spectrum,[2] a number of bands were observed coincident with Raman frequencies, and this apparent violation of the mutual exclusion rule was ascribed to lowered symmetry, possibly D_3, in the crystals. A strong band at 570 cm^{-1} which was not coincident with any Raman frequency could confidently be assigned to F_{1u}. An additional noncoincident band, at 325 cm^{-1}, was also assigned to F_{1u}. However we have not been able to fit this frequency into the calculations using reasonable force constants. The intensity of the band is similar to that of the symmetry-forbidden bands, and it might reasonably arise from a vibration inactive under O_h, but rendered active by the proposed crystalline distortion. On the other hand, our calculations do predict an F_{1u} mode at about 420 cm^{-1}. There is considerable absorption in this region (see Figure 2 of ref 2) but it is obscured by the symmetry-forbidden bands at 406 and 434 cm^{-1}. It seems likely that these ride on top of the unobserved F_{1u} mode. The infrared spectrum below 170 cm^{-1} showed only a broad, featureless absorption, in which the remaining F_{1u} modes may have been hidden. Lattice modes and Raman modes made active in the crystal are also candidates for this region.

Normal Coordinate Analysis

F and G matrices for octahedral $Bi_6(OH)_{12}^{6+}$ (neglecting hydrogen atoms) were constructed according to Wilson, Decius, and Cross,[5] using the interatomic distances given by Danforth, *et al.*[4] These parameters were determined in solution, but in the absence of a crystallographic determination we assume that they are valid for the perchlorate crystals as well, on the basis of the close similarity of the Raman spectra in the two phases. The internal coordinates are defined in Figure 1, and symmetry coordinates formed from them are given in Table I. Table II lists the contributions of the internal coordinates and the redundancy conditions in each symmetry class. The G matrix elements were calculated with a computer program developed by Schachtschneider,[6] SD-4064.

The force constants defined in Table III were combined to form the symmetry F matrix elements listed in Table IV. Solution of the secular equation, with least-squares refinement of the force constants, was carried out with a computer program also developed by Schachtschneider,[6] SD-4032. Our initial trial, involving a force field containing only a metal–oxygen stretching constant and bond-bending constants for the structural angles α and β, defined in Figure 1, was unsuccessful. The addition to this force field of stretch–stretch interactions of the metal–oxygen bonds greatly improved the agreement between observed and calculated frequencies for the bands above 200 cm^{-1}, but the fit for bands below 200 cm^{-1} was still inadequate. Only when an off-diagonal element for stretch–bend interaction at the Bi–O–Bi angle was added could a satisfactory fit for all of the observed frequencies be obtained. This result is given under calculation I in Table V.

With this force field eight observed frequencies are calculated successfully using six parameters. The unobserved F_{2g} mode and one of the unobserved F_{1u} modes are calculated to have zero frequency due to neglect of a bending force constant for the angle γ. Addition of small values of H_γ to this field led to calculated values for these modes which are too low in frequency to be observed in our spectra. The addition of H_γ had no effect on the other force constants and an examination of the G matrix elements involving the angle γ showed that

(5) E. B. Wilson, J. C. Decius, and P. C. Cross, "Molecular Vibrations," McGraw-Hill Book Co., Inc., New York, N. Y., 1955.

(6) R. G. Snyder and J. H. Schachtschneider, *Spectrochim. Acta*, **19**, 117 (1963).

TABLE I

SYMMETRY COORDINATES FOR $Bi_6(OH)_{12}^{6+}$ [a]

A_{1g}

$$S_r^{(A_{1g})} = \frac{1}{\sqrt{24}}[r(1,10) + r(1,7) + r(1,11) + r(1,17) + r(2,13) + r(2,8) + r(2,9) + r(2,15) + r(3,18) + r(3,17) + r(3,16) + r(3,15) + r(4,14) + r(4,11) + r(4,12) + r(4,13) + r(5,9) + r(5,10) + r(5,14) + r(5,18) + r(6,7) + r(6,8) + r(6,12) + r(6,16)]$$

$$S_\alpha^{(A_{1g})} = \frac{1}{\sqrt{12}}[\alpha(10,1,7) + \alpha(11,1,17) + \alpha(9,2,8) + \alpha(15,2,13) + \alpha(17,3,15) + \alpha(18,3,16) + \alpha(11,4,13) + \alpha(12,4,14) + \alpha(10,5,9) + \alpha(18,5,14) + \alpha(7,6,8) + \alpha(12,6,16)]$$

$$S_\beta^{(A_{1g})} = \frac{1}{\sqrt{12}}[\beta(1,7,6) + \beta(1,10,5) + \beta(6,8,2) + \beta(2,9,5) + \beta(1,11,4) + \beta(2,13,14) + \beta(2,15,3) + \beta(1,17,3) + \beta(3,18,5) + \beta(4,14,5) + \beta(4,12,6) + \beta(3,16,6)]$$

$$S_\gamma^{(A_{1g})} = \frac{1}{\sqrt{24}}[\gamma(10,1,17) + \gamma(11,1,7) + \gamma(7,1,17) + \gamma(10,1,11) + \gamma(9,2,13) + \gamma(9,2,15) + \gamma(8,2,13) + \gamma(8,2,15) + \gamma(15,3,16) + \gamma(16,3,17) + \gamma(17,3,18) + \gamma(15,3,18) + \gamma(11,4,12) + \gamma(12,4,13) + \gamma(13,4,14) + \gamma(11,4,14) + \gamma(9,5,18) + \gamma(9,5,14) + \gamma(10,5,14) + \gamma(10,5,18) + \gamma(7,6,16) + \gamma(7,6,12) + \gamma(8,6,16) + \gamma(8,6,12)]$$

$$S_D^{(A_{1g})} = \frac{1}{\sqrt{12}}[D(1,6) + D(2,6) + D(2,5) + D(1,5) + D(1,3) + D(1,4) + D(2,3) + D(2,4) + D(3,5) + D(3,6) + D(4,5) + D(4,6)]$$

E_g

$$S_{r(1)}^{(E_g)} = \frac{1}{\sqrt{48}}[2r(1,10) + 2r(1,7) + 2r(2,9) + 2r(2,8) + 2r(5,9) + 2r(5,10) + 2r(6,7) + 2r(6,8) - r(1,11) - r(1,17) - r(2,13) - r(2,15) - r(3,15) - r(3,16) - r(3,17) - r(3,18) - r(4,11) - r(4,12) - r(4,13) - r(4,14) - r(5,14) - r(5,18) - r(6,12) - r(6,16)]$$

$$S_{r(3)}^{(E_g)} = \frac{1}{\sqrt{4}}[r(1,11) + r(1,17) + r(2,13) + r(2,15) + r(5,14) + r(5,18) + r(6,12) + r(6,16) - r(3,15) - r(3,16) - r(3,17) - r(3,18) - r(4,11) + r(4,12) - r(4,13) - r(4,14)]$$

$$S_{\alpha(1)}^{(E_g)} = \frac{1}{\sqrt{8}}[\alpha(11,1,17) + \alpha(13,3,15) + \alpha(14,5,18) + \alpha(12,6,16) - \alpha(15,3,17) - \alpha(16,3,18) - \alpha(11,4,13) - \alpha(12,4,14)]$$

$$S_{\alpha(2)}^{(E_g)} = \frac{1}{\sqrt{24}}[2\alpha(7,1,10) + 2\alpha(8,2,9) + 2\alpha(9,5,10) + 2\alpha(7,6,8) - \alpha(11,1,17) - \alpha(13,2,15) - \alpha(15,3,17) - \alpha(16,3,18) - \alpha(11,4,13) - \alpha(12,4,14) - \alpha(12,6,16) - \alpha(14,5,18)]$$

$$S_\beta^{(E_g)} = \frac{1}{\sqrt{24}}[2\beta(1,7,6) + 2\beta(1,10,5) + 2\beta(2,8,6) + 2\beta(2,9,5) - \beta(1,11,4) - \beta(1,17,3) - \beta(2,13,4) - \beta(2,15,3) - \beta(3,16,6) - \beta(3,18,5) - \beta(4,12,6) - \beta(4,14,5)]$$

$$S_\gamma^{(E_g)} = \frac{1}{\sqrt{48}}[2\gamma(15,3,16) + 2\gamma(15,3,18) + 2\gamma(16,3,17) + 2\gamma(17,3,18) + 2\gamma(11,4,12) + 2\gamma(11,4,14) + 2\gamma(12,4,13) + 2\gamma(13,4,14) - \gamma(7,1,11) - \gamma(7,1,17) - \gamma(10,1,17) - \gamma(10,1,11) - \gamma(8,2,13) - \gamma(8,2,15) - \gamma(9,2,13) - \gamma(9,2,15) - \gamma(9,5,14) - \gamma(9,5,18) - \gamma(10,5,14) - \gamma(10,5,18) - \gamma(7,6,12) - \gamma(7,6,16) - \gamma(8,6,12) - \gamma(8,6,16)]$$

$$S_D^{(E_g)} = \frac{1}{\sqrt{24}}[2D(1,5) + 2D(1,6) + 2D(2,5) + 2D(2,6) - D(1,3) - D(1,4) - D(2,3) - D(2,4) - D(3,5) - D(3,6) - D(4,5) - D(4,6)]$$

F_{2g}

$$S_r^{(F_{2g})} = \frac{1}{\sqrt{24}}[r(1,7) + r(1,17) + r(2,9) + r(2,13) + r(3,16) + r(3,17) + r(4,13) + r(4,14) + r(6,7) + r(6,16) + r(5,9) + r(5,14) - r(1,10) - r(1,11) - r(2,8) - r(2,15) - r(3,15) - r(3,18) - r(4,11) - r(4,12) - r(5,10) - r(5,18) - r(6,8) - r(6,12)]$$

$$S_\alpha^{(F_{2g})} = 0 \text{ (α does not contribute to } F_{2g})$$

$$S_\beta^{(F_{2g})} = \frac{1}{\sqrt{12}}[\beta(1,7,6) + \beta(1,17,3) + \beta(3,16,6) + \beta(2,9,5) + \beta(2,13,4) + \beta(4,14,5) - \beta(1,10,5) - \beta(1,11,4) - \beta(2,8,6) - \beta(2,15,3) - \beta(3,18,5) - \beta(4,12,6)]$$

$$S_{\gamma(1)}^{(F_{2g})} = \frac{1}{\sqrt{12}}[\gamma(7,1,17) + \gamma(7,6,16) + \gamma(16,3,17) - \gamma(10,1,11) - \gamma(15,3,18) - \gamma(8,6,12) + \gamma(9,2,13) + \gamma(13,4,14) + \gamma(9,5,14) - \gamma(8,2,15) - \gamma(11,4,12) - \gamma(10,5,18)]$$

$$S_{\gamma(2)}^{(F_{2g})} = \frac{1}{\sqrt{24}}[\gamma(7,1,17) + \gamma(7,6,16) + \gamma(16,3,17) + \gamma(10,1,11) + \gamma(15,3,18) + \gamma(8,6,12) + \gamma(8,2,15) + \gamma(9,2,13) + \gamma(9,5,14) + \gamma(10,5,18) + \gamma(11,4,12) + \gamma(13,4,14) - \gamma(10,1,17) - \gamma(11,1,7) - \gamma(8,2,13) - \gamma(9,2,15) - \gamma(15,3,16) - \gamma(17,3,18) - \gamma(11,4,14) - \gamma(12,4,13) - \gamma(9,5,18) - \gamma(10,5,14) - \gamma(7,6,12) - \gamma(8,6,16)]$$

$$S_D^{(F_{2g})} = \frac{1}{\sqrt{12}}[D(1,3) + D(1,6) + D(3,6) + D(2,4) + D(2,5) + D(4,5) - D(1,4) - D(1,5) - D(2,3) - D(2,6) - D(3,5) - D(4,6)]$$

F_{1u}

$$S_{r(1)}^{(F_{1u})} = \frac{1}{\sqrt{24}}[r(1,7) + r(1,10) + r(1,11) + r(1,17) + r(3,15) + r(3,16) + r(3,17) + r(3,18) + r(6,7) + r(6,8) + r(6,12) + r(6,16) - r(2,8) - r(2,9) - r(2,13) - r(2,15) - r(4,11) - r(4,12) - r(4,13) - r(4,14) - r(5,9) - r(5,10) - r(5,14) - r(5,18)]$$

$$S_{r(2)}^{(F_{1u})} = \frac{1}{\sqrt{24}}[r(1,7) + r(1,17) + r(3,16) + r(3,7) + r(6,7) + r(6,16) - r(1,10) - r(1,11) - r(3,15) - r(3,18) - r(6,8) - r(6,12) - r(2,9) - r(2,13) - r(4,13) - r(4,14) - r(5,9) - r(5,14) + r(2,8) + r(2,15) + r(4,11) + r(4,12) + r(5,10) + r(5,18)]$$

$$S_\alpha^{(F_{1u})} = \frac{1}{\sqrt{12}}[\alpha(7,1,10) + \alpha(11,1,17) + \alpha(15,3,17) + \alpha(16,3,18) + \alpha(7,6,8) + \alpha(12,6,16) - \alpha(8,2,9) - \alpha(13,2,15) - \alpha(11,4,13) - \alpha(12,4,14) - \alpha(9,5,10) - \alpha(14,5,18)]$$

$$S_\beta^{(F_{1u})} = \frac{1}{\sqrt{6}}[\beta(1,7,6) + \beta(1,17,3) + \beta(3,16,6) - \beta(2,9,5) - \beta(2,13,4) - \beta(4,14,5)]$$

$$S_{\gamma(1)}^{(F_{1u})} = \frac{1}{\sqrt{24}}[\gamma(7,1,11) + \gamma(7,1,17) + \gamma(10,1,11) + \gamma(10,1,17) + \gamma(15,3,16) + \gamma(15,3,18) + \gamma(16,3,17) + \gamma(17,3,18) + \gamma(7,6,12) + \gamma(7,6,16) + \gamma(8,6,12) + \gamma(8,6,16) - \gamma(8,2,13) - \gamma(8,2,15) - \gamma(9,2,13) - \gamma(9,2,15) - \gamma(11,4,12) - \gamma(11,4,14) - \gamma(12,4,13) - \gamma(13,4,14) - \gamma(9,5,14) - \gamma(9,5,18) - \gamma(10,5,14) - \gamma(10,5,18)]$$

$$S_{\gamma(2)}^{(F_{1u})} = \frac{1}{\sqrt{12}}[\gamma(7,1,17) + \gamma(16,3,17) + \gamma(7,6,16) - \gamma(10,1,11) - \gamma(15,3,18) - \gamma(8,6,12) + \gamma(8,2,15) + \gamma(11,4,12) + \gamma(10,5,18) - \gamma(9,2,13) - \gamma(9,5,14) - \gamma(13,4,14)]$$

$$S_D^{(F_{1u})} = \frac{1}{\sqrt{6}}[D(1,3) + D(1,6) + D(3,6) - D(2,5) - D(2,4) - D([4,5)]$$

[a] Symbols: r, α, β, γ, D = internal coordinates defined in Figure 1. Numbers in parentheses refer to atoms connected by the internal coordinates, following the numbering system in Figure 1.

this angle would contribute substantially only to F_{2g} and F_{1u} modes.

The valence force constants adjusted in this manner must be considered to be quite approximate, in view of the necessarily simplified force field used, and the neglect of the hydrogen atoms, intermolecular forces, and anharmonicity. Comparisons with related molecules should still be useful, however. The metal–oxygen stretching constant of 1.65 mdyn/Å is a little low compared, for example, with the value of 2.21 mdyn/Å which has been reported for $Zn(OH)_4^{2-}$.[7] The bond-bending constants are somewhat larger than expected, their usual order of magnitude being less than one-tenth of the stretching force constant.[8] The magnitudes of the stretch–stretch interactions about the metal atom, k' and k'', are likewise somewhat larger than expected. These are also commonly of the order of one-tenth of the stretching force constant.[9] The potential energy distribution obtained from calculation I, given in Table VI, shows considerable mixing of the bond-stretching and bond-bending coordinates in most of the normal modes.

The X-ray scattering measurements of Danforth,

(7) E. R. Lippincott, J. A. Psellos, and M. C. Tobin, *J. Chem. Phys.*, **20**, 536 (1952).

(8) See ref 5, p 177.

(9) See ref 5, p 178.

TABLE II

CONTRIBUTIONS OF THE INTERNAL COORDINATES TO THE NORMAL MODES FOR $Bi_6(OH)_{12}^{6+}$

Internal coordinate	No. of contributions to each symmetry class			
	A_{1g}	E_g	F_{2g}	F_{1u}
r	1	2	1	2
α	1	2	0	1
β	1	1	1	1
γ	1	1	2	2
D	1	1	1	1

Redundancy conditions

A_{1g}

$$S_\alpha^{(A_{1g})} + S_\beta^{(A_{1g})} = 0$$

$$S_\beta^{(A_{1g})} + 5.3707 S_\gamma^{(A_{1g})} = 0$$

$$1.1247 S_r^{(A_{1g})} - 7.5887 S_\gamma^{(A_{1g})}) - S_D^{(A_{1g})} = 0$$

E_g

$$1.1547 S_\beta^{(E_g)} + 0.5773 S_{\alpha(1)}^{(E_g)} - S_{\alpha(2)}^{(E_g)} = 0$$

$$0.9119 S_{r(1)}^{(E_g)} - 0.4020 S_{r(2)}^{(E_g)} + 1.6456 S_\beta^{(E_g)} + S_{\alpha(1)}^{(E_g)} = 0$$

$$-0.1862 S_{\alpha(1)}^{(E_g)} + S_\gamma^{(E_g)} = 0$$

$$-0.3413 S_{r(1)}^{(E_g)} - 0.3448 S_{r(2)}^{(E_g)} + 4.606 S_\gamma^{(E_g)} + S_D^{(E_g)} = 0$$

F_{2g}

$$0.6773 S_r^{(F_{2g})} + 0.9825 S_\beta^{(F_{2g})} - 0.7071 S_{\gamma(1)}^{F(2g)} + S_{\gamma(2)}^{(F_{2g})} = 0$$

$$-0.1048 S_r^{(F_{2g})} + 0.6958 S_\beta^{(F_{2g})} - 0.7071 S_{\gamma(1)}^{(F_{2g})} + S_{\gamma(2)}^{(F_{2g})} = 0$$

F_{1u}

$$0.0006 S_{r(1)}^{(F_{1u})} - 0.0004 S_{r(2)}^{(F_{1u})} - 5.3769 F_{\gamma(1)}^{(F_{1u})} + S_\alpha^{(F_{1u})} = 0$$

$$0.3443 S_{r(1)}^{(F_{1u})} + 0.2634 S_{r(2)}^{(F_{1u})} + 4.3106 S_{\gamma(1)}^{(F_{1u})} + S_\beta^{(F_{1u})} = 0$$

$$-0.6379 S_{r(1)}^{(F_{1u})} + 0.3721 S_{r(2)}^{(F_{1u})} + 6.0886 S_{\gamma(1)}^{(F_{1u})} + S_D^{(F_{1u})} = 0$$

TABLE III

FORCE CONSTANTS

Symbol	Description of interaction
K	Bi–O stretch
H_α	O–Bi–O bend at angle α
H_β	Bi–O–Bi bend at angle β
H_γ	O–Bi–O bend at angle γ
k'	Stretch–stretch interaction at angle γ
k''	Stretch–stretch interaction at angle α
k'''	Stretch–stretch interaction at angle β
k_β	Stretch–bend interaction at angle β
D	Bi–Bi stretch

TABLE IV

NONZERO SYMMETRY F MATRIX ELEMENTS

A_{1g}

$$F_{rr} = K + 2k' + k'' + k'''$$
$$F_{r\beta} = \sqrt{2}k_\beta$$
$$F_{\alpha\alpha} = H_\alpha$$
$$F_{\beta\beta} = H_\beta$$
$$F_{\gamma\gamma} = H_\gamma$$
$$F_{DD} = D$$

E_g

$$F_{r(1)r(1)} = K - k' + k'' + k'''$$
$$F_{r(2)r(2)} = K + k' - k'''$$
$$F_{r(1)r(2)} = \sqrt{3}k'$$
$$F_{r(1)\beta} = \sqrt{2}k_\beta$$
$$F_{\alpha(1)\alpha(1)} = H_\alpha$$
$$F_{\alpha(2)\alpha(2)} = H_\alpha$$
$$F_{\beta\beta} = H_\beta$$
$$F_{\gamma\gamma} = H_\gamma$$
$$F_{DD} = D$$

F_{2g}

$$F_{rr} = K - k'' + k'''$$
$$F_{r\beta} = \sqrt{2}k_\beta$$
$$F_{\beta\beta} = H_\beta$$
$$F_{\gamma(1)\gamma(1)} = H_\gamma$$
$$F_{\gamma(2)\gamma(2)} = H_\gamma$$
$$F_{DD} = D$$

F_{1u}

$$F_{r(1)r(1)} = K + 2k' + k''$$
$$F_{r(2)r(2)} = K - k''$$
$$F_{r(1)r(2)} = k'''$$
$$F_{r(1)\beta} = k_\beta$$
$$F_{r(2)\beta} = \frac{1}{\sqrt{2}}k_\beta$$
$$F_{\alpha\alpha} = H_\alpha$$
$$F_{\beta\beta} = H_\beta$$
$$F_{\gamma(1)\gamma(1)} = H_\gamma$$
$$F_{\gamma(2)\gamma(2)} = H_\gamma$$
$$F_{DD} = D$$

TABLE V

SUMMARY OF VIBRATIONAL CALCULATIONS FOR $Bi_6(OH)_{12}^{6+}$

Species	Obsd	Calcn I	Calcn II	Calcn III	Calcn IV
	Frequencies, cm^{-1}				
A_{1g}	450	450	450	451	456
	177	177	183	176	177
E_g	434	434	434	434	436
	262	262	262	268	260
	90	95	89	88	89
F_{2g}	406	406	406	404	397
	108	107	97	113	115
	a	0	0	0	0
F_{1u}	570	570	570	570	569
	b	410	413	420	421
	a	180	186	148	149
	a	0	0	0	0
	Force constants, mdyn/Å				
K	1.647	1.800	1.762	1.770	
k'	0.304	0.324	0.436	0.406	
k''	−0.414	−0.377	*c*	*c*	
k'''	*c*	*c*	−0.060	−0.353	
H_α	0.237	0.271	*c*	*c*	
H_β	0.328	0.292	*c*	*c*	
H_γ	*c*	*c*	*c*	*c*	
k_β	0.254	0.336	*c*	*c*	
D	*c*	*c*	0.965	0.967	

[a] Not observed. [b] Not resolved. [c] Not included in the calculation.

TABLE VI

POTENTIAL ENERGY DISTRIBUTION

Normal mode freq, cm^{-1}	Calculation I				Calculation II	
	V_{rr}[a]	$V_{r\beta}$	$V_{\alpha\alpha}$	$V_{\beta\beta}$	V_{rr}	V_{DD}
570 (F_{1u})	85	−3	13	5	100	0
450 (A_{1g})	64	−53	37	52	100	0
434 (E_g)	26	−15	52	27	100	0
420 (F_{1u})	95	−49	8	46	99	1
406 (F_{2g})	117	−66	0	49	98	2
262 (E_g)	196	−185	33	56	100	0
117 (A_{1g})	51	25	10	14	0	100
108 (F_{2g})	6	19	0	75	2	98
90 (E_g)	8	−5	47	50	0	100
180 (F_{1u})	36	16	33	15	...	...
148 (F_{1u})	...	...	...	...	1	99

[a] $V_{i,j}$ = normalized contribution to the potential energy from F matrix elements of the type (i, j).

et al.,[4] give an accurate estimate of the bismuth–bismuth distances in $Bi_6(OH)_{12}^{6+}$, but the lighter oxygen atoms are located much less accurately. In order to determine how sensitive our calculation was to the uncertainty in the oxygen positions, we reconstructed the G matrix using a metal–oxygen bond lengthened by 0.16 Å. (The half-width of the Bi–O peak in the radial distribution function of Danforth, *et al.*, is about 0.3 Å.) The force constants obtained with this adjusted G matrix are given under calculation II in Table V. The resultant changes are fairly small, indicating that the force field is not seriously affected by uncertainty in the oxygen positions. The potential energy distribution for this calculation varied insignificantly from that for calculation I.

We next modified the force field by introducing a valence force between bismuth atoms, to replace the

restoring forces at the angles α and β. The three observed frequencies below 200 cm^{-1} could now be fit remarkably well using a single Bi–Bi stretching force constant, D. For a good fit in the high-frequency region stretch–stretch interaction constants still had to be retained along with the primary Bi–O stretching force constant. The result is given as calculation III in Table V. In this force field the interaction k'' is replaced by a small value for k'''. The predicted zero frequency for the unobserved F_{2g} mode and one of the unobserved F_{1u} mode results, as before, from neglect of H_γ. Eight observed frequencies are now reproduced with four parameters.

The potential energy distribution resulting from this calculation, given in Table VI, shows a distinct separation of the internal coordinates for Bi–O stretching and Bi–Bi stretching in all of the modes. The Bi–Bi interaction is essentially the sole contributor to the modes below 200 cm^{-1}, while Bi–O stretching accounts quantitatively for the modes above 200 cm^{-1}. The calculated Bi–O stretching force constant is not much different from that obtained in calculation I. The magnitude of the metal–metal stretching constant is about half that found for Hg_2^{2+},[10] *ca.* 1.93 mdyn/Å.

Finally, using the new force field we carried out the same variation as before of the G matrix, by increasing the Bi–O distance by 0.16 Å. The result is given as calculation IV in Table V. The effect of the G matrix variation is very small for all of the force constants except k''', which is increased by a factor of about six. The potential energy distribution remains essentially unaltered.

Discussion

From the foregoing analysis we conclude that the vibrational spectrum of $Bi_6(OH)_{12}^{6+}$ is indeed in quantitative accord with the structure proposed by Danforth, *et al.*, if reasonable valence forces are assumed. The calculation is not very sensitive to the uncertainty in the positions of the oxygen atoms, its influence being mostly absorbed in the interaction constants. If the force field is drawn up on the assumption that bonding occurs only between bismuth and oxygen atoms, then the internal coordinates are highly mixed in the various normal modes. If a bismuth–bismuth interaction is introduced into the force field, the spectrum can be fit with fewer parameters, and there is a dramatic separation of internal coordinates in the normal modes.

The question remains whether the bismuth–bismuth interaction is real or whether it is merely a formal device which serves by accident to simplify a force field which is in fact quite complicated. The main evidence on this point relates to the anomalously high intensity of the low-frequency Raman bands (see Figure 1 of ref 2). If it is assumed that the bonding electrons in the complex are located entirely in the bismuth–oxygen bonds, then one would expect the high-frequency vibrations, which involve primarily bismuth–oxygen stretching, to produce larger polarizability changes and therefore higher Raman intensities than the low-frequency vibrations, which have a higher admixture of bond bending. In fact, the intensities are the other way around, the bands below 200 cm^{-1} being considerably more intense than those above 200 cm^{-1}. However, in the force field with bismuth–bismuth interaction, the low-frequency bands are due almost entirely to bismuth–bismuth stretching. If there were significant electron density in bismuth–bismuth bonds, these modes would involve a considerable polarizability change and their high intensity would thereby be explained. In particular, of the two A_{1g} bands, the one at 177 cm^{-1} is much more intense than the one at 450 cm^{-1}. Both are totally symmetric "breathing" vibrations of the complex, the latter involving primarily motion in and out of the oxygen atoms, and the former involving primarily motion in and out of the bismuth atoms, the oxygen atoms riding along with them. It is difficult to understand why the low-frequency motion should produce a polarizability change greater than the high-frequency motion unless significant electron density is delocalized in the cage of the bismuth atoms. On the basis of these intensity considerations we feel that the analysis in terms of bismuth–bismuth interactions may well have some physical reality behind it.

There is considerable current interest in metal–metal bonds in inorganic compounds. These are well characterized in species such as the mercurous ion dimer or dimanganese decacarbonyl, where the only contact is between the metals. For species in which the metals are bridged by other atoms the situation is always more controversial and the relevant evidence is indirect. Most commonly the distance between the metal atoms is used as a guide, distances comparable to those found in the pure metal being considered indicative of bonding. Even for zerovalent metal atoms, however, this is apparently a rather restrictive standard, since the metal–metal distance in dimanganese decacarbonyl is considerably greater then that found in metallic manganese.[11] For metals in higher oxidation states the situation is still less certain. The bismuth atoms in $Bi_6(OH)_{12}^{6+}$, while substantially farther apart, 3.71 Å, then in the metal, 3.10 Å, may nevertheless be in close enough proximity to allow some overlap of atomic orbitals. The bonds under consideration are quite weak.

Cotton and Haas[12] have devised a molecular orbital scheme for $Ta_6Cl_{12}^{2+}$, to which $Bi_6(OH)_{12}^{6+}$ is structurally analogous. However the main feature of their scheme, overlap of metal d orbital, is inappropriate here because the 5d level of Bi(III) is filled and the 6d level is high in energy. The highest filled and lowest unfilled Bi(III) orbitals are 6s and 6p, respectively. The energy gap between them is substantial (8.8 ev in the free ion[13]) and the s electrons are generally con-

(10) H. M. Gager, J. Lewis, and M. J. Ware, *Chem. Commun.*, 616 (1966).

(11) L. F. Dahl, E. Ishishi, and R. E. Rundle, *J. Chem. Phys.*, **26**, 1750 (1957).

(12) F. A. Cotton and T. E. Haas, *Inorg. Chem.*, **3**, 10 (1964).

(13) C. E. Moore, "Atomic Energy Levels," Vol. III, Circular No. 467, National Bureau of Standards, U. S. Government Printing Office, Washington, D. C., 1958.

sidered to be "inert." Nevertheless, a degree of hybridization of s and p orbitals would be favored if the energy so expended were counterbalanced by electrostatic stabilization as suggested by Orgel,[14] or through overlap of the resulting hybrids to form bonding orbitals. If we allow hybridization of bismuth s and p_z orbitals on $Bi_6(OH)_{12}^{6+}$ (z is taken as the direction on each bismuth toward the center of the cage), the resulting hybrids would be favorably oriented for mutual overlap. They would form a bonding set of six molecular orbitals, inside the Bi_6 cage, in which the twelve bismuth valence electrons could be delocalized, and a corresponding antibonding set outside the cage.

The bismuth p_x and p_y orbitals would then be left for bonding with the hydroxyl oxygens. Twelve bonding molecular orbitals would thus be available for 24 of the hydroxyl electrons. Two filled orbitals on each oxygen would be left nonbonding. This arrangement is equivalent to a set of twelve three-center O–Bi–O bonds. The predicted average metal–oxygen bond order is one-half, and this may explain the somewhat low value for the Bi–O stretching constant. Twelve three-center metal–ligand bonds are also called for in the equivalent orbital scheme for the $Ta_6Cl_{12}^{2+}$ cage proposed by Kettle.[15] However his use of eight face-centered orbitals for metal–metal bonding is inapplicable to Bi(III).

A possible energy level scheme based on these considerations is sketched out in Figure 2. Here bismuth ions (A) are allowed to hybridize individually (B), come together in an octahedral array (C), and then combine with hydroxyl ions (D). The ordering of energy levels is far from unambiguous, but it seems profitless at this time to undertake a quantitative calculation. Since the 6p–6d separation in Bi(III) is not much larger than the 6s–6p separation,[13] a more complete description would have to consider mixing in of bismuth d orbitals as well. However our purpose here is merely to indicate that weak bismuth–bismuth bonding may be a reasonable feature of the electronic structure of $Bi_6(OH)_{12}^{6+}$.

Acknowledgment.—We are indebted to Professors Niel Bartlett and William DeW. Horrocks for invaluable discussions of our results. This work made use of computer facilities supported in part by National Science Foundation Grant NSF-GP579.

(14) L. E. Orgel, *J. Chem. Soc.*, 3815 (1959).

(15) S. F. A. Kettle, *Theoret. Chim. Acta*, **3**, 211 (1965).

CONTRIBUTION FROM THE DEPARTMENT OF CHEMISTRY,
PRINCETON UNIVERSITY, PRINCETON, NEW JERSEY 08540

Vibrational Analysis for Polynuclear Hydroxylead(II) Complexes[1a]

BY VICTOR A. MARONI[1b] AND THOMAS G. SPIRO

Received June 13, 1967

The vibrational spectrum of $Pb_4(OH)_4^{4+}$ has been subjected to a normal coordinate analysis, based on a tetrahedral structure for this species, using the known Pb–Pb and Pb–O distances in solution. Agreement with experiment was readily obtained, but only if an attractive interaction between lead atoms was included in the force field. For the complex containing 1.33 hydroxides per lead, whose composition is probably $Pb_6(OH)_8^{4+}$, the presumption of an octahedral structure is supported by the observation of three low-frequency Raman bands at frequency ratios found to be characteristic of metal cages of cubic symmetry. A vibrational analysis based on this structure and the assumption that the Pb–Pb and Pb–O distances are the same as for $Pb_4(OH)_4^{4+}$ led to an excellent fit of the data with force constants similar to those used for $Pb_4(OH)_4^{4+}$. Evidence for lead–lead bonding in these complexes is provided by the anomalously high intensity observed for the low-frequency Raman bands attributable to the lead cages. A bonding scheme similar to that proposed[2] for $Bi_6(OH)_{12}^{6+}$ can be applied.

Introduction

The previous article[2] described a normal coordinate analyses for the $Bi_6(OH)_{12}^{6+}$ cuboctahedron. The main conclusion reached was that the Raman spectrum could best be understood on the basis of direct, if weak, bonding among the bismuth atoms. In the present work we continue our spectroscopic studies of hydroxymetal polyhedra, with an analysis of the vibrational spectra of polynuclear lead complexes, which were recently reported.[3] The results parallel those obtained for $Bi_6(OH)_{12}^{6+}$, Raman spectra again providing evidence for weak metal–metal bonding.

Lead(II) is isoelectronic with bismuth(III) and both hydrolyze to give soluble complexes, whose structures are however quite different. Bismuth produces the octahedral hexamer $Bi_6(OH)_{12}^{6+}$ while the main product of lead hydrolysis is a tetramer, $Pb_4(OH)_4^{4+}$. Its structure, as deduced by Esval[4] from solution X-ray scattering measurements, is a distorted cube consisting of lead and oxygen atoms arranged tetrahedrally, as shown in Figure 1. The Raman spectrum of per-

(1) (a) This investigation was supported by Public Health Service Grant GM-13498, from the National Institute of General Medical Sciences; (b) NASA Predoctoral Fellow.

(2) V. A. Maroni and T. G. Spiro, *Inorg. Chem.*, **7**, 183 (1968).

(3) V. A. Maroni and T. G. Spiro, *J. Am. Chem. Soc.*, **89**, 45 (1967).

(4) O. E. Esval, Thesis, University of North Carolina, 1962.